

# Direct spin accumulation quantification in ferromagnetic heterostructures using DC bias harmonic Hall measurement

H. Y. Poh , C. C. I. Ang , W. L. Gan, G. J. Lim, and W. S. Lew \*

*School of Physical and Mathematical Sciences, Nanyang Technological University, 21 Nanyang Link, Singapore 637371*



(Received 14 September 2021; accepted 23 November 2021; published 13 December 2021)

A technique for spin accumulation quantification, specifically in the ferromagnetic layer of spin-orbit torque inducing heterostructures has been elusive. Here, we demonstrate an easy-to-implement technique to achieve this quantification by applying an additional DC bias during the harmonic Hall measurement in Si/SiO<sub>2</sub>/Ta/Co/Pt. The spin accumulation arising from the DC bias generates an amplitude offset detectable in the first harmonic Hall magnetoresistance. By performing the first harmonic Hall magnetoresistance measurement under a fixed DC bias for two oppositely magnetized states, spin accumulation polarity set by the DC bias enhances the magnetoresistance if it aligns with the magnetization, and vice versa. Thus, the difference in the magnetoresistance amplitude provides the quantitative magnitude of spin accumulation relative to the ferromagnet's saturation magnetization, measured to be up to 0.29% in Si/SiO<sub>2</sub>/Ta/Co/Pt. The strength of both spin accumulation and dampinglike efficiency increased with Ta thickness, further verifying our experimental technique.

DOI: [10.1103/PhysRevB.104.224416](https://doi.org/10.1103/PhysRevB.104.224416)

## I. INTRODUCTION

The spin Hall effect (SHE) manifests as the conversion of electrical charge current flowing through a metallic material into a transverse spin current due to the effect of spin-dependent scattering [1–3]. The spin scattering leads to the accumulation of spins along the lateral edges of the metallic layer. If a heavy metal (HM) layer is used and is interfaced with a ferromagnetic (FM) layer, the accumulated spins diffuse from the HM layer into the FM layer. The injected spins exchange angular momentum with the local magnetization within the FM layer [4–10], inducing the spin-orbit torque (SOT) effect. It is crucial to define a metric that describes and quantifies the spins accumulated within the FM layer, which determines the SOT strength. Characterization of spin accumulation in the HM layer has been reported using longitudinal magnetic-optic Kerr effect (MOKE) technique [3,11–14]. However, due to the existence of spin backflow, where the spins are reflected back into the HM layer [15], and spin memory loss, where the spin flips beyond the spin diffusion length [16,17], quantification of the net spins that diffused into the FM layer from the HM layer is remained unsolved, specifically for FM/HM bilayer structure. In addition, as the optical signal detected from spin accumulation is relatively small, spatial imaging is challenging and the resolution is limited by the optical diffraction limit [18]. Although x-ray magnetic circular dichroism (XMCD) allows direct quantification of spin accumulation in the ferromagnetic layer in HM/FM structure [18–20], this setup is not easily accessible as it requires the need of synchrotron facility. Therefore, a robust and easily-accessible characterization technique that can directly quantify the spin accumulation in the FM layer

has been a subject of continued pursuit in the effort of understanding the SOT mechanism.

In this work, we demonstrate direct electrical detection of spin accumulation in the Co layer in a Si/SiO<sub>2</sub>/Ta/Co/Pt structure with in-plane magnetic anisotropy (IMA) using harmonic Hall measurement technique with a direct current (DC) bias. The inclusion of the DC bias results in an anomalous resistance originating from spin accumulation induced by the SHE. The sign of this anomalous resistance is dependent on the accumulated spins being parallel or antiparallel to the local magnetization. A correlation between the quantified spin accumulation and the dampinglike term was determined in a Ta thickness-dependent study. Our electrical measurement approach opens up an avenue for direct measurement of spin accumulation in the FM layer, which can potentially be more sensitive and accurate as compared to MOKE microscopy, while being more accessible as compared to XMCD.

## II. MODEL

The harmonic Hall measurement technique quantifies two mutually orthogonal components of the SOT: Dampinglike field  $\mathbf{H}_D = H_D \mathbf{m} \times \mathbf{p}$  and fieldlike field,  $\mathbf{H}_F = H_F \mathbf{p}$ , where  $\mathbf{p}$  is the polarized spin orientation of electrons [5,6,21–26]. In this technique, sweeping field and alternating current are applied to induce first and second harmonic Hall resistance,  $R_\omega$  and  $R_{2\omega}$  respectively. The  $R_\omega$  provides information about the equilibrium magnetization direction and the  $R_{2\omega}$  provides information about the SOT-induced small tilting of magnetization from the equilibrium via the planar Hall effect (PHE) and anomalous Hall effect [24–28]. With the inclusion of spin accumulation that is induced by SHE by applied DC, it will result in an increase / decrease in PHE.

The direction of the accumulated spin is dependent on the direction of the current flow and the sign of characteristic

\*Corresponding author: [wensiang@ntu.edu.sg](mailto:wensiang@ntu.edu.sg)

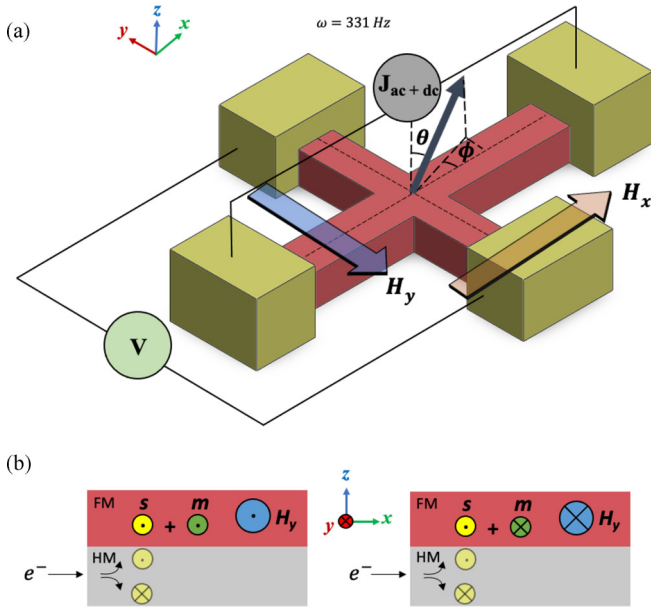


FIG. 1. (a) Schematic of DC bias harmonic Hall setup in the longitudinal configuration. (b) Schematic of the spin accumulation in the FM/HM structure with in-plane anisotropy. Spins are accumulated in the  $+\hat{y}$  direction in the FM layer when the injected electron is in the  $+\hat{x}$  direction. Local magnetization,  $\mathbf{m}$  follows the direction of the external field,  $H_y$ . The amplitude of first Harmonics resistance,  $R_\omega$  increases (decreases) when spin accumulations,  $s$ , are parallel (antiparallel) to the local magnetization of the FM layer as described in Eq (2).

material spin Hall angle,  $\theta_H$ . This can be described by  $\hat{s} = (\hat{v} \times \hat{n} (\theta_H))$ , where  $\hat{s}$  is the direction of the accumulated spin,  $\hat{v}$  is the direction of electron flow, and  $\hat{n}$  is the surface normal. Given the current flow in the  $+\hat{x}$ -direction and structure with positive spin Hall angle, such as Pt, the electrons are scattered towards the top/bottom interface while being polarized in the  $\pm\hat{y}$  direction. Therefore, we propose that the spin accumulation will manifest as a change in the planar Hall resistance in the  $\hat{y}$  direction. The  $R_\omega$  for an IMA structure can be expressed as  $R_\omega = R_p \sin 2\phi$ , where  $R_p$  is planar Hall resistance which is proportional to  $m_x m_y$ , and  $\phi$  is the azimuthal angle as shown in Fig. 1(a). Due to the accumulation of spins in the  $\hat{y}$  direction, the  $R_\omega$  is given by

$$R_\omega = r_p(m_x \cdot (m_y + s)) \sin 2\phi, \quad (1)$$

$$R_\omega = (R_p + \Delta R_p) \sin 2\phi, \quad (2)$$

where  $r_p$  is the coefficient of planar Hall resistance,  $\Delta R_p$  is the additional planar Hall resistance due to spin accumulation, and  $s$  is the spin accumulation. The quantification of spin accumulation was measured by a harmonic Hall measurement with DC bias, applying DC concurrently with the adiabatic AC along the Hall cross structure. The alignment of the magnetization in the  $\hat{y}$ -direction can be fixed by the external magnetic field,  $\pm H_y$ . The polarity of  $H_y$  will not affect  $\Delta R_p$  since the polarity of accumulated spins is only dependent on the direction of current flow. By applying  $\pm H_y$ , the magnitudes of  $R_\omega$  are expected to be different due to the direction of the accumulated spins.  $\Delta R_p$  is obtained by

summing up these values of  $R_\omega(\pm H_y)$ . This can be written as  $\Delta R_p = \frac{R_\omega(+H_y) + R_\omega(-H_y)}{2}$ . The spin accumulation is then determined by the ratio between  $\Delta R_p$  and  $R_p$ . The applied DC bias is substantial to induced the thermoelectric effect,  $V_{TE}$ , however, this effect is accounted for and found to be negligible. The sign  $V_{TE}$  is dependent on the magnetization ( $\mathbf{m} \times \nabla T$ ) where  $\nabla T$  is the temperature gradient due to Joule heating in the  $\hat{x}$  and  $\hat{z}$  directions [29,30]. Since the sweeping field is in  $\hat{x}$  direction, the first harmonic Hall voltage due to  $V_{TE}$  will be cancelled out due to the opposite signs of  $m_y$ . Hence, the  $V_{TE}$  has been eliminated in the quantification of the spin accumulation.

Since the spin accumulation quantification in our model is dependent on  $\Delta R_p$ , it is primarily applicable to IMA structures, where the spins and initial magnetization are parallel / antiparallel to each other. For the case for PMA materials, the Hall voltage signal is dominated by the anomalous Hall effect, leaving negligible  $\Delta R_p$  signal.

### III. MEASUREMENT AND RESULTS

#### A. Characterization of SOT field in Ta/Co/Pt

Harmonic Hall measurements were carried out on a Si/SiO<sub>2</sub>/Ta(2 nm)/Co(2 nm)/Pt(5 nm) Hall cross structure to characterize the SOT efficiency. The thin film stack was deposited using DC magnetron sputtering, and subsequently patterned into a  $5 \times 20 \mu\text{m}$  Hall cross structure using a combination of optical lithography and ion milling techniques. Vibrating sample magnetometer measurement shows that the film stack has IMA with saturation magnetization,  $M_s = 650 \pm 18 \text{ emu/cc}$  [31]. The harmonic Hall technique was used to obtain the  $R_\omega$  and  $R_{2\omega}$  with respect to the azimuthal angle of magnetization  $\phi = \arctan \frac{H_y}{H_x}$ , where  $H_x$  is the fixed external magnetic field of 600 Oe, and  $H_y$  is the sweeping magnetic field ranging from  $-4000 \text{ Oe}$  to  $4000 \text{ Oe}$ . Uniform AC densities,  $j_{ac}$  ranging from  $1 \times 10^{11} \text{ A/m}^2$  to  $1.5 \times 10^{11} \text{ A/m}^2$  were applied in the  $\hat{x}$  direction to obtain the dampinglike efficiency.  $H_D$  is determined from  $R_{2\omega}$  using [32]:

$$R_{2\omega} = R_A \frac{H_D}{2H_s} X + R_p \frac{H_F}{H_{x_{\text{ext}}}} (2X^4 - X^2), \quad (3)$$

where  $X = \cos \phi$  and  $H_s$  is the saturation field.  $H_D$  is plotted against the electric field,  $E$  as shown in Fig. 2(b), and the electric field can be obtained by  $E = \rho_{xx} \mathbf{j}$ , where  $\rho_{xx}$  is the resistivity of the structure, and  $\mathbf{j}$  is the uniform current density flowing into the structure. The dependence on electric field is preferred over uniform current density because the different resistivities of the layer will result in different current densities within the constituents of the trilayer. The uniform current density flowing into the trilayer will be less than the current density in Pt, resulting in overestimating the SOT efficiency. In addition, there are more than one source generating SOT, it is experimentally impractical to isolate the individual SOT efficiency.

The SOT dampinglike efficiency,  $\zeta_{DL}^E$  can be calculated by  $\zeta_{DL}^E = \frac{\mu_0 M_s t H_D}{E}$  [33], where  $\mu_0$  is the permeability of vacuum, and  $t$  is the thickness of the FM layer. The results for the  $R_{2\omega}$  and  $\zeta_{DL}^E$  for Si/SiO<sub>2</sub>/Ta/Co/Pt are shown in Fig. 2(c). The  $\zeta_{DL}^E$  increased from  $(20.05 \pm 0.07) \times 10^5 (\Omega \text{ m})^{-1}$  to

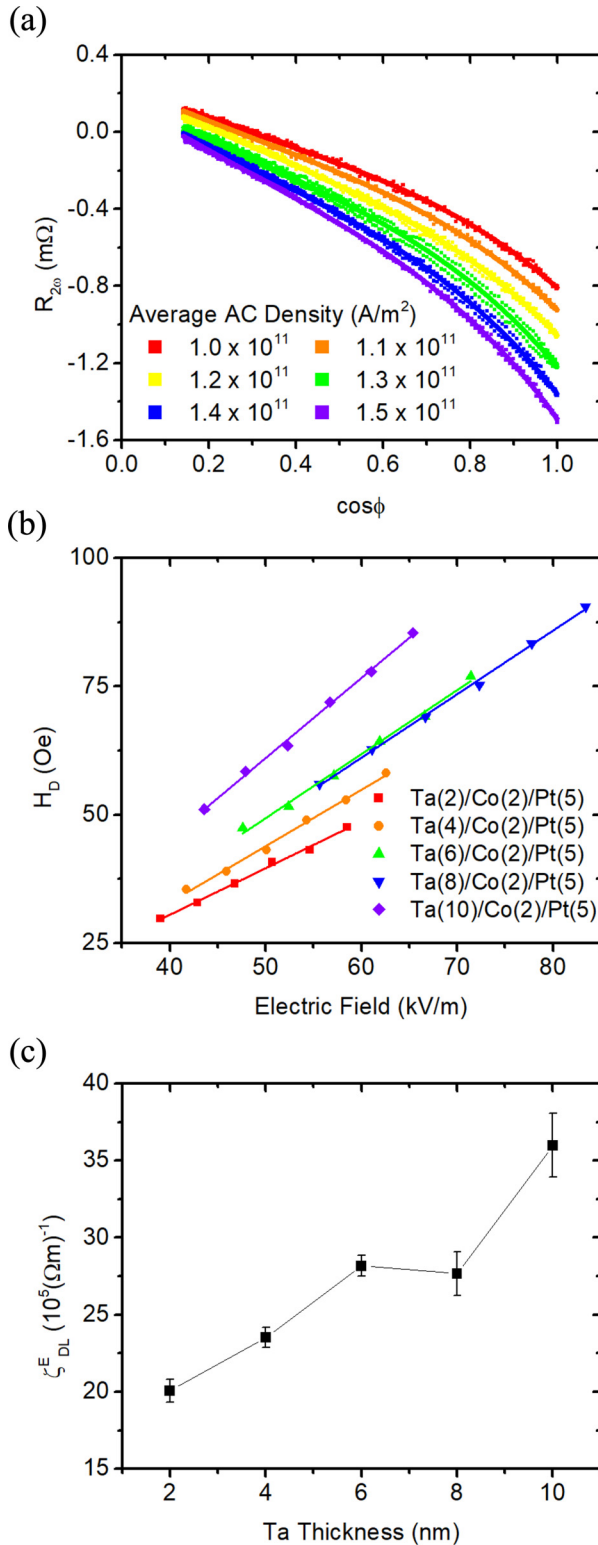


FIG. 2. (a)  $R_{2\omega}$  as a function of  $\cos\phi$ , for average current density ranging from  $1-1.5 \times 10^{10} A/m^2$ . Graph of  $AX + B(2X^4 - X^2)$  is fitted to the data. (b)  $H_D$  as a function of electric field for various Ta thicknesses ranging from 2 to 10 nm. (c)  $\zeta_{DL}^E$  as a function of Ta thickness.

$(35.99 \pm 2.07) \times 10^5 (\Omega m)^{-1}$  when the thickness of Ta is increased from 2 to 10 nm. This is because increasing the

thickness of Ta will increase the percentage content of  $\beta$ -phase Ta which had been reported for higher contribution of SOT [34–36]. The magnitude of these  $\zeta_{DL}^E$  correspond to approximately the effective spin Hall angle of 0.138 to 0.276 ( $\theta_H^{eff} = \frac{2eM_s t H_D}{\hbar j}$ ) under the assumption of uniform current density injection through the trilayer structure which are comparable to various other reports [32,34,37–39].

### B. Quantification of spin accumulation

In order to quantify the spin accumulation in the FM layer, a uniform AC current density,  $j_{ac} = 5.0 \times 10^{10}$   $A/m^2$  with a DC offset,  $j_{dc} = 5.0 \times 10^{10}$   $A/m^2$  was injected through the trilayer structure in a longitudinal scheme with respect to the sweeping field.  $R_{\omega}$  was measured under a sweeping magnetic field of  $\pm 1000$  Oe in the  $\hat{x}$  direction and a fixed magnetic field of 600 Oe in the  $\hat{y}$  direction. As seen in Eq. (2), the amplitude of  $R_{\omega}$  determines the total planar Hall resistance ( $R_p + \Delta R_p$ ). The experimental results show that  $R_p$  is measured to be 63.2  $m\Omega$  for zero DC bias; meanwhile, the total planar Hall resistances are 62.7  $m\Omega$  and  $-64.0$   $m\Omega$  for  $+H_y$  and  $-H_y$ , respectively with DC offset as illustrated in Fig. 3(a). Therefore, we can conclude that the spin of the electrons are polarized in the  $-\hat{y}$  direction in the FM layer. With the presence of DC bias, the polarized spins are aligned parallel (antiparallel) to the localized magnetization of the FM, leading to an increase (decrease) in total magnetization, as illustrated in Fig. 1(b). Without an applied DC ( $j_{DC} = 0$ ), there will be no net accumulated spin. Hence, the amplitude of the  $R_{\omega}$  between  $+H_y$  and  $-H_y$  is expected to be the same. The  $\Delta R_p$  is obtained by summing the amplitude of  $R_{\omega}$  for  $\pm H_y$ . A linear trend in  $\Delta R_p$  is observed from the sweeping  $j_{DC}$  from  $1 \times 10^{10}$   $A/m^2$  to  $5 \times 10^{10}$   $A/m^2$ . Thus, a linear fit is used to determine the rate of change of  $\Delta R_p$  per electric field as shown in Fig. 3(b). From the gradient of the linear fit, the spin accumulation is calculated by  $s = \frac{1}{R_p} \frac{d\Delta R_p}{dE}$ .

To both confirm that the SHE is the dominant source resulting in spin accumulation and an increase in spin accumulation would lead to a larger  $\Delta R_p$ , measurements were performed on samples with Ta thickness ranging from 2 to 10 nm. The measurement results of spin accumulation in the Co layer with varying Ta thickness are shown in Fig. 4. Factoring in the  $M_s$  of the Hall structure, the obtained spin accumulation results are  $1.19 \times 10^{17} \mu_B/cm^3$  per V/m and  $2.05 \times 10^{17} \mu_B/cm^3$  per V/m, for Ta = 2 nm and Ta = 10 nm, respectively. In addition, a similar trend of spin accumulation and the  $\zeta_{DL}^E$  with Ta thickness in Si/SiO<sub>2</sub>/Ta/Co/Pt is observed, as shown in Fig. 4. The Rashba effect is an interfacial effect, which is independent of the HM thickness, whereas SHE is a bulk effect which is dependent on the HM thickness. These results further affirm the dominance of the SHE in our stack structures, which is the cause of spin accumulation building up in the FM layer. To quantify the degree of influence in spin accumulation on the FM layer, the measured spin accumulation is normalized to the saturation magnetization of the FM layer, and a value of 0.29% per kV/m in Co for Si/SiO<sub>2</sub>/Ta(10)/Co(2)/Pt(5) is obtained.

The measurement was repeated on another IMA sample of Si/SiO<sub>2</sub>/Ti(2)/Co(2)/Pt(5) with Ti ranging from 2 to 10 nm. Since Ti was reported to have a low dampinglike term, it

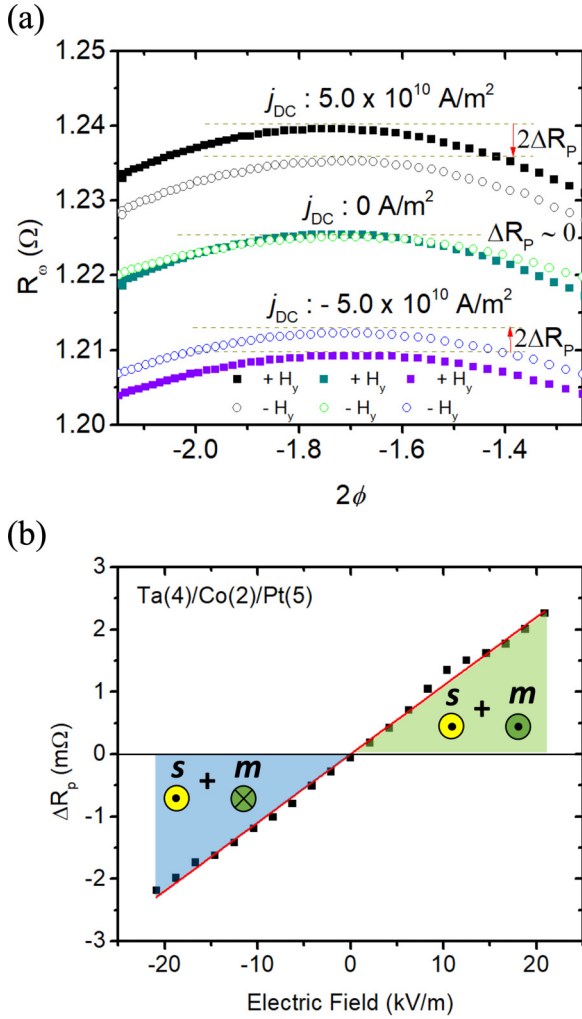


FIG. 3. (a)  $R_\omega$  for  $+H_y$  (solid square) and  $-H_y$  (open circle). Offsets have been applied to the  $R_\omega$  for better clarity.  $R_\omega$  for  $-H_y$  is flipped for a clearer comparison. Spin accumulation is parallel (antiparallel) to  $+H_y$  ( $-H_y$ ), leading to a higher amplitude in the  $R_\omega$  at the current density of  $j_{DC} = 5.0 \times 10^{10} \text{ A/m}^2$ . (b) Amplitude of  $\Delta R_p$  with respect to the electric field. The slope of  $\Delta R_p$  over electric field is  $0.11 \text{ m}\Omega \text{ per kV/m}$ .

will be intriguing to determine how the spin accumulation changes with the dampinglike efficiency. The results of the spin accumulation and dampinglike efficiency are shown in Fig. 4. Spin accumulation of  $2.09 \times 10^{16} \mu_B/\text{cm}^3$  per  $\text{V/m}$  was obtained for the Si/SiO<sub>2</sub>/Ti(2)/Co(2)/Pt(5) sample. To align the unit of spin accumulation measurement so as to make comparison with reported values, our measured spin accu-

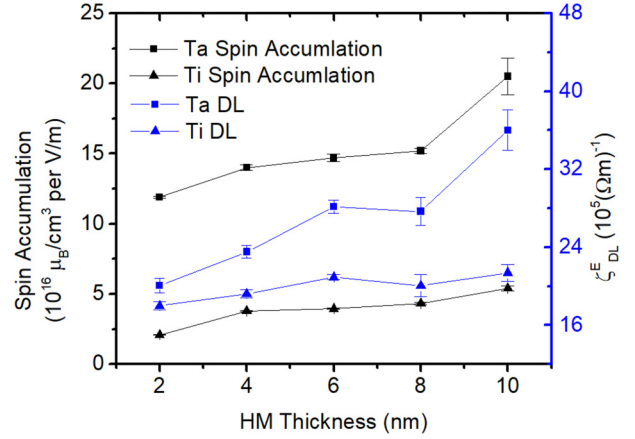


FIG. 4. Spin accumulation of Ta (black square) and Ti (black triangle), and DL efficiency of Ta (blue square) and Ti (black triangle) with various HM thicknesses ranging from 2 to 10 nm.

mulation in Si/SiO<sub>2</sub>/Ti/Co/Pt is in the range  $1.55 \times 10^{-4} \sim 2.09 \times 10^{-4} \mu_B/\text{atom}$  per  $10^6 \text{ A/cm}^2$ . This value is comparable to  $\sim 1.75 \times 10^{-4} \mu_B/\text{atom}$  per  $10^6 \text{ A/cm}^2$ , which is measured by XMCD in Co/Pt structure [19]. The measured spin accumulation from Ti,  $s_{Ti}$  is lower than spin accumulation from Ta,  $s_{Ta}$ . This further shows that spin accumulation is proportional to the dampinglike efficiency.

#### IV. CONCLUSION

In conclusion, current-induced spin accumulation in Si/SiO<sub>2</sub>/Ta/Co/Pt and Si/SiO<sub>2</sub>/Ti/Co/Pt structures have been quantified using the harmonic Hall measurement technique with DC bias. Our experiments show that the spin accumulation is approximately 0.29% per  $\text{kV/m}$  of the local magnetization for 10 nm Ta. Our results demonstrate that, besides the conventional SOT measurement, spin accumulation can also be quantified using the harmonic Hall technique. The ratio of the spin accumulation over the applied electric field shows a similar trend with dampinglike efficiency as the thickness of HM increases. Hence, the ratio can be used to evaluate the efficiency of an HM in converting electric current to spin current. This provides an all-electrical alternative to determine spin accumulation by utilizing the easily accessible harmonic Hall characterization technique.

#### ACKNOWLEDGMENT

This work was supported by RIE2020 ASTAR AME IAF-ICP Grant No. I1801E0030 and EDB-IPP (Grant No. RCA-2019-1376).

- [1] J. Sinova, S. O. Valenzuela, J. Wunderlich, C. H. Back, and T. Jungwirth, Spin Hall effects, *Rev. Mod. Phys.* **87**, 1213 (2015).  
 [2] S. Murakami and N. Nagaosa, Spin Hall effect, *Compr. Semicond. Sci. Technol.* **1-6**, 222 (2011).

- [3] C. Stamm, C. Murer, M. Berritta, J. Feng, M. Gabureac, P. M. Oppeneer, and P. Gambardella, Magneto-Optical Detection of the Spin Hall Effect in Pt and W Thin Films, *Phys. Rev. Lett.* **119**, 087203 (2017).

- [4] A. Manchon and S. Zhang, Theory of spin torque due to spin-orbit coupling, *Phys. Rev. B* **79**, 094422 (2009).
- [5] T. D. Skinner, K. Olejník, L. K. Cunningham, H. Kurebayashi, R. P. Campion, B. L. Gallagher, T. Jungwirth, and A. J. Ferguson, Complementary spin-hall and inverse spin-galvanic effect torques in a ferromagnet/semiconductor bilayer, *Nat. Commun.* **6**, 4 (2015).
- [6] S. Emori, U. Bauer, S. M. Ahn, E. Martinez, and G. S. D. Beach, Current-driven dynamics of chiral ferromagnetic domain walls, *Nat. Mater.* **12**, 611 (2013).
- [7] S. O. Valenzuela and M. Tinkham, Direct electronic measurement of the spin hall effect, *Nature (London)* **442**, 176 (2006).
- [8] M. I. Dyakonov and V. I. Perel, Current-induced spin orientation of electrons in semiconductors, *Phys. Lett. A* **35**, 459 (1971).
- [9] I. M. Miron, K. Garello, G. Gaudin, P. J. Zermatten, M. V. Costache, S. Auffret, S. Bandiera, B. Rodmacq, A. Schuhl, and P. Gambardella, Perpendicular switching of a single ferromagnetic layer induced by in-plane current injection, *Nature (London)* **476**, 189 (2011).
- [10] X. Fan, H. Celik, J. Wu, C. Ni, K. J. Lee, V. O. Lorenz, and J. Q. Xiao, Quantifying interface and bulk contributions to spin-orbit torque in magnetic bilayers, *Nat. Commun.* **5**, 3042 (2014).
- [11] F. Fohr, S. Kaltenborn, J. Hamrle, H. Schultheiß, A. A. Serga, H. C. Schneider, B. Hillebrands, Y. Fukuma, L. Wang, and Y. Otani, Optical Detection of Spin Transport in Nonmagnetic Metals, *Phys. Rev. Lett.* **106**, 226601 (2011).
- [12] G. M. Choi, Magneto-optical kerr effect driven by spin accumulation on Cu, Au, and Pt, *Appl. Sci.* **8**, 1378 (2018).
- [13] V. Sih, R. C. Myers, Y. K. Kato, W. H. Lau, A. C. Gossard, and D. D. Awschalom, Spatial imaging of the spin hall effect and current-induced polarization in two-dimensional electron gases, *Nat. Phys.* **1**, 31 (2005).
- [14] P. Riego, S. Vélez, J. M. Gomez-Perez, J. A. Arregi, L. E. Hueso, F. Casanova, and A. Berger, Absence of detectable current-induced magneto-optical kerr effects in Pt, Ta, and W, *Appl. Phys. Lett.* **109**, 172402 (2016).
- [15] K. Hashimoto, G. Tatara, and C. Uchiyama, Spin backflow: A non-markovian effect on spin pumping, *Phys. Rev. B* **99**, 205304 (2019).
- [16] K. Chen and S. Zhang, Spin Pumping in the Presence of Spin-Orbit Coupling, *Phys. Rev. Lett.* **114**, 126602 (2015).
- [17] J. Borge and I. V. Tokatly, Ballistic spin transport in the presence of interfaces with strong spin-orbit coupling, *Phys. Rev. B* **96**, 115445 (2017).
- [18] J. Ding, W. Zhang, M. B. Jungfleisch, J. E. Pearson, H. Ohldag, V. Novosad, and A. Hoffmann, Direct observation of spin accumulation in cu induced by spin pumping, *Phys. Rev. Res.* **2**, 2 (2020).
- [19] C. Stamm, C. Murer, Y. Acremann, M. Baumgartner, R. Gort, S. Däster, A. Kleibert, K. Garello, J. Feng, M. Gabureac, Z. Chen, J. Stöhr, and P. Gambardella, X-ray spectroscopy of current-induced spin-orbit torques and spin accumulation in Pt/3d -transition-metal bilayers, *Phys. Rev. B* **100**, 024426 (2019).
- [20] R. Kukreja, S. Bonetti, Z. Chen, D. Backes, Y. Acremann, J. A. Katine, A. D. Kent, H. A. Dürr, H. Ohldag, and J. Stöhr, X-Ray Detection of Transient Magnetic Moments Induced by a Spin Current in Cu, *Phys. Rev. Lett.* **115**, 096601 (2015).
- [21] I. M. Miron, G. Gaudin, S. Auffret, B. Rodmacq, A. Schuhl, S. Pizzini, J. Vogel, and P. Gambardella, Current-driven spin torque induced by the rashba effect in a ferromagnetic metal layer, *Nat. Mater.* **9**, 230 (2010).
- [22] K. Garello, I. M. Miron, C. O. Avci, F. Freimuth, Y. Mokrousov, S. Blügel, S. Auffret, O. Boulle, G. Gaudin, and P. Gambardella, Symmetry and magnitude of spin-orbit torques in ferromagnetic heterostructures, *Nat. Nanotechnol.* **8**, 587 (2013).
- [23] X. Wang and A. Manchon, Diffusive Spin Dynamics in Ferromagnetic Thin Films with a Rashba Interaction, *Phys. Rev. Lett.* **108**, 117201 (2012).
- [24] J. Kim, J. Sinha, M. Hayashi, M. Yamanouchi, S. Fukami, T. Suzuki, S. Mitani, and H. Ohno, Layer thickness dependence of the current-induced effective field vector in ta[CoFeB]MgO, *Nat. Mater.* **12**, 240 (2013).
- [25] M. Jamali, K. Narayanapillai, X. Qiu, L. M. Loong, A. Manchon, and H. Yang, Spin-Orbit Torques in Co/Pd Multilayer Nanowires, *Phys. Rev. Lett.* **111**, 246602 (2013).
- [26] M. Hayashi, J. Kim, M. Yamanouchi, and H. Ohno, Quantitative characterization of the spin-orbit torque using harmonic hall voltage measurements, *Phys. Rev. B* **89**, 144425 (2014).
- [27] P. P. J. Haazen, E. Murè, J. H. Franken, R. Lavrijsen, H. J. M. Swagten, and B. Koopmans, Domain wall depinning governed by the spin hall effect, *Nat. Mater.* **12**, 299 (2013).
- [28] X. Qiu, W. Legrand, P. He, Y. Wu, J. Yu, R. Ramaswamy, A. Manchon, and H. Yang, Enhanced Spin-Orbit Torque via Modulation of Spin Current Absorption, *Phys. Rev. Lett.* **117**, 217206 (2016).
- [29] E. S. Park, D. K. Lee, B. C. Min, and K. J. Lee, Elimination of thermoelectric artifacts in the harmonic hall measurement of spin-orbit torque, *Phys. Rev. B* **100**, 214438 (2019).
- [30] H. Yang, H. Chen, M. Tang, S. Hu, and X. Qiu, Characterization of spin-orbit torque and thermoelectric effects via coherent magnetization rotation, *Phys. Rev. B* **102**, 024427 (2020).
- [31] Q. Y. Wong, C. Murapaka, W. C. Law, W. L. Gan, G. J. Lim, and W. S. Lew, Enhanced Spin-Orbit Torques in Rare-Earth Pt/[Co/Ni] 2/Co/Tb Systems, *Phys. Rev. Appl.* **11**, 24057 (2019).
- [32] F. Luo, S. Goolaup, W. C. Law, S. Li, F. Tan, C. Engel, T. Zhou, and W. S. Lew, Simultaneous determination of effective spin-orbit torque fields in magnetic structures with in-plane anisotropy, *Phys. Rev. B* **95**, 174415 (2017).
- [33] L. Zhu, D. C. Ralph, and R. A. Buhrman, Enhancement of spin transparency by interfacial alloying, *Phys. Rev. B* **99**, 180404 (2019).
- [34] S. Woo, M. Mann, A. J. Tan, L. Caretta, and G. S. D. Beach, Enhanced spin-orbit torques in Pt /Co / Ta heterostructures enhanced spin-orbit torques in Pt / Co / Ta heterostructures, *Appl. Phys. Lett.* **105**, 212404 (2016).
- [35] L. Liu, C. F. Pai, Y. Li, H. W. Tseng, D. C. Ralph, and R. A. Buhrman, Spin-torque switching with the giant spin hall effect of tantalum, *Science* **336**, 555 (2012).
- [36] G. Allen, S. Manipatruni, D. E. Nikonov, M. Doczy, and I. A. Young, Experimental demonstration of the coexistence of spin hall and rashba effects in  $\beta$ -tantalum/ferromagnet bilayers, *Phys. Rev. B* **91**, 144412 (2015).
- [37] C. Hahn, G. De Loubens, O. Klein, M. Viret, V. V. Naletov, and J. Ben Youssef, Comparative measurements of inverse spin hall effects and magnetoresistance in YIG/Pt and YIG/Ta, *Phys. Rev. B* **87**, 174417 (2013).

- [38] F. Luo, Q. Y. Wong, S. Li, F. Tan, G. J. Lim, X. Wang, and W. S. Lew, Dependence of spin-orbit torque effective fields on magnetization uniformity in Ta/Co/Pt structure, *Sci. Rep.* **9**, 10776 (2019).
- [39] S. Woo, M. Mann, A. Tan, L. Carreta, and G. Beach, Characterization of Spin-Orbit Torques in Pt/Co/Ta Structures, 2015 IEEE International Magnetics Conference (INTERMAG), 2015, pp. 1–1, doi: [10.1109/INTMAG.2015.7156653](https://doi.org/10.1109/INTMAG.2015.7156653).